EVOLUTIONARY BIOLOGY

How genomic insights into the evolutionary history of clouded leopards inform their conservation

Jiaqing Yuan¹†, Guiqiang Wang¹†, Le Zhao^{1,2}†, Andrew C. Kitchener^{3,4}†, Ting Sun¹, Wu Chen⁵, Chen Huang¹, Chen Wang⁵, Xiao Xu¹, Jinhong Wang¹, Huimeng Lu⁶, Lulu Xu¹, Qigao Jiangzuo⁷, William J. Murphy⁸, Dongdong Wu⁹*, Gang Li^{1,5}*

Clouded leopards (*Neofelis* spp.), a morphologically and ecologically distinct lineage of big cats, are severely threatened by habitat loss and fragmentation, targeted hunting, and other human activities. The long-held poor understanding of their genetics and evolution has undermined the effectiveness of conservation actions. Here, we report a comprehensive investigation of the whole genomes, population genetics, and adaptive evolution of *Neofelis*. Our results indicate the genus *Neofelis* arose during the Pleistocene, coinciding with glacial-induced climate changes to the distributions of savannas and rainforests, and signatures of natural selection associated with genes functioning in tooth, pigmentation, and tail development, associated with clouded leopards' unique adaptations. Our study highlights high-altitude adaptation as the main factor driving nontaxonomic population differentiation in *Neofelis nebulosa*. Population declines and inbreeding have led to reduced genetic diversity and the accumulation of deleterious variation that likely affect reproduction of clouded leopards, highlighting the urgent need for effective conservation efforts.

Copyright © 2023 True
Authors, some
rights reserved;
exclusive licensee
American Association
for the Advancement
of Science. No claim to
original U.S. Government
Works. Distributed
under a Creative
Commons Attribution
NonCommercial
License 4.0 (CC BY-NC).

INTRODUCTION

The two extant clouded leopard species, *Neofelis nebulosa* and *Neofelis diardi*, are the closest living relatives to the five big cats of the genus *Panthera*, and, together, they form the subfamily Pantherinae (1, 2). Clouded leopards (Fig. 1A) are highly adapted to an arboreal lifestyle. They have broad paws, a long tail to maintain balance, and flexible ankles that can rotate nearly 180°, allowing them to descend trees headfirst (3). Compared to all other extant felids, clouded leopards also have the largest upper canine teeth in proportion to body size (4); their canines are similar in proportion to those of some extinct sabertooth cats. Despite their large upper canines, clouded leopards do not kill their prey with a canine shear bite (5) such as the sabretooths but, instead, use a crushing nape bite such as extant large felids.

Whereas the evolutionary history of *Panthera* is characterized by frequent intercontinental migrations (6, 7), the historical range of *Neofelis* is restricted to Southeast Asia, from the eastern Himalayas to Sundaland (1, 2). Formerly recognized as a monospecifc genus, *Neofelis* is now known to comprise two species. The mainland clouded leopard (MCL), *N. nebulosa*, is distributed in Nepal, India, South China, and the Indochinese Peninsula, while the

¹College of Life Sciences, Shaanxi Normal University, Xi'an, China. ²QinLing-Bashan Mountains Bioresources Comprehensive Development C. I. C., School of Bioscience and Engineering, Shaanxi University of Technology, Hanzhong, China. ³Department of Natural Sciences, National Museums Scotland, Chambers Street, Edinburgh EH1 1JF, UK. ⁴School of Geosciences, University of Edinburgh, Drummond Street, Edinburgh EH9 3PX, UK. ⁵Guangzhou Zoo, Guangzhou Wildlife Research Center, Guangzhou, China. ⁶School of Life Sciences, Northwestern Polytechnical University, Xi'an, China. ⁷Key Laboratory of Vertebrate Evolution and Human Origins of Chinese Academy of Sciences, Institute of Vertebrate Paleontology and Paleoanthropology, Chinese Academy of Sciences, Beijing, China. ⁸Veterinary Integrative Biosciences, Texas A&M University, College Station, TX, USA. ⁹State Key Laboratory of Genetic Resources and Evolution, Kunming Natural History Museum of Zoology Kunming Institute of Zoology, Chinese Academy of Sciences, Kunming, China.

*Corresponding author. Email: gli@snnu.edu.cn (G.L.); wudongdong@mail.kiz.ac. cn (D.W.)

Sunda clouded leopard (SCL), *N. diardi*, is currently restricted to the two islands of Borneo and Sumatra. The estimated population size of the MCL ranges from 3700 to 5580 (8), while the SCL population is estimated at 4500 (9). The MCL has been subdivided into three subspecies: *N. nebulosa nebulosa* (*N. n. nebulosa*) (southern China and Indochinese Peninsula), *N. nebulosa macrosceloides* (*N. n. macrosceloides*) (northeast India and Nepal), and *N. nebulosa brachyurus* (*N. n. brachyurus*) from Taiwan that may extinct in recent decades (1).

Clouded leopards are found only in tropical forests and have lost more than 30% of their habitat over the past two decades (10), and both species are listed by the IUCN (https://www.iucnredlist.org/) as vulnerable (9). Habitat loss and fragmentation and illegal wildlife trade (11) have led to profound and well-documented genetic depletion in other felids (12, 13), but little is known about these impacts on the genetics of clouded leopards. Ex situ conservation efforts have been impeded by the high incidence of pleomorphic spermatozoa and pathogen transmission from domestic animals in captivity (14). Understanding the clouded leopards' evolutionary history and genetic diversity can potentially promote more effective conservation efforts by providing information about the selective pressures important to the evolution and adaptation of the two known extant species and identifying negative genetic consequences of ancient to modern demographic history. Here, we generated a chromosome-level reference genome of the MCL and carried out comparative genomics aimed at revealing the genomic signatures underpinning the unique morphological adaptions of both species. We reconstruct their demographic history to investigate the occurrence of population bottlenecks during the origin and population differentiation of clouded leopards associated with palaeoclimatic changes in south Asia. We also investigate losses in genetic diversity and the accumulation of deleterious mutations, which may pose challenges for the future management of these species both in the wild and in the captivity.

[†]These authors contributed equally to this work.

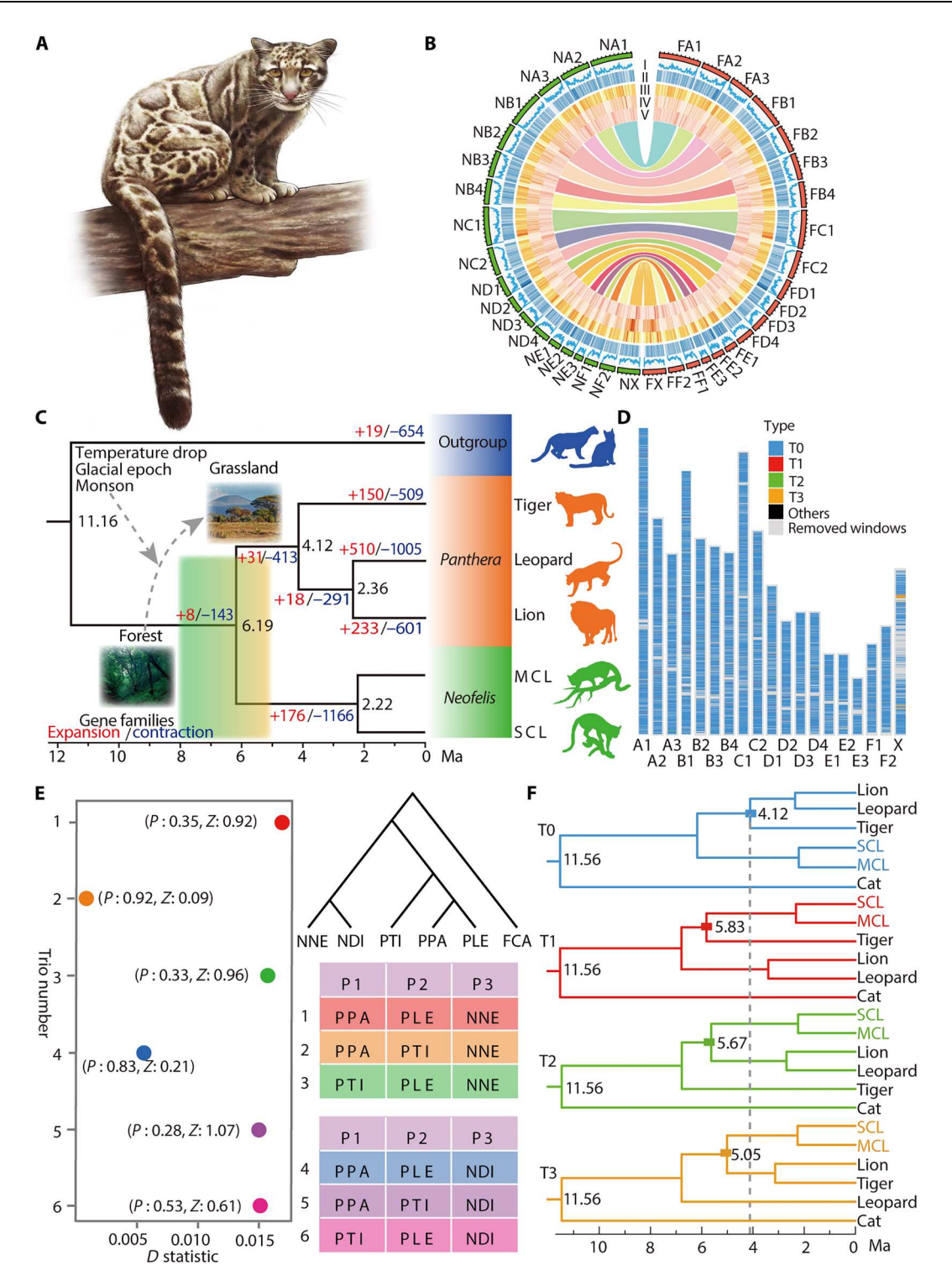


Fig. 1. Results of genome assembly and phylogenomic tests of clouded leopard. (A) An MCL. (B) Circos plot of chromosome alignment between clouded leopard (left) and domestic cat (right). The comparisons include gas chromatography content (I), gene density (II), repetitive elements [III: Short interspersed nuclear element (SINE), IV: Long interspersed nuclear elements (LINE), and V: Long terminal repeats (LTR)], and the inner curves of genome collinearity in 20-kb sliding windows. (C) Phylogenomic reconstruction and estimated divergence times (black numbers near each node) of genera *Neofelis* and *Panthera*. The expanded and contracted gene families (red and blue numbers) are shown near each branch. (D) Distribution of the genomic phylogenetic discordance across each chromosome of *Neofelis* tested by 50-kb sliding windows. The different colors represent the variable phylogenetic topologies of T0 to T3 shown in (E). (E) Topologies of the four most frequent sliding trees of T0 to T3 with estimated divergent times. NNE, *Neofelis nebulosa*; NDI, *Neofelis diardi*; FCA, *Felis catus*. (F) The introgression test between *Neofelis* and tiger [*Panthera tigris* (PTI)], leopard [*Panthera pardus* (PPA)], and lion [*Panthera leo* (PLE)]. Different colors marked six "trios" tests from 1 to 6.

RESULTS AND DISCUSSION

Genomic data

We sequenced the genome of a female N. nebulosa (20 N. nebulosa samples in table S1) using 175 gigabytes (GB) of Oxford Nanopore Technology long reads, 70 gigabytes of Illumina paired-end short reads, and 120 gigabytes of Hi-C reads to generate a high-quality de novo genome assembly. We also sequenced the genome of a female N. diardi using 80 gigabytes of Illumina reads that were used in a variety of analyses to gain insights into different aspects of clouded leopard genetics and evolutionary history. These analyses included phylogenomic analysis, divergence time estimation, tests for introgression or incomplete lineage sorting (ILS), investigations into adaptive evolution, genomic diversity analysis, and population genetics analysis. Each of these approaches used advanced methods and techniques to examine and interpret the genomic data obtained from the sequencing reads. For the population genetics analysis, we performed whole-genome resequencing of 20 N. nebulosa samples gathered from museum collections and wild or captive living individuals (table S1), which produced 1.2 terabytes (TB) of Illumina short-read data. The average sequencing depth of each sample was 25.5×, covering more than 99% of genome regions. A total of 4.16 million high-quality single-nucleotide polymorphisms (SNPs) from all 20 samples were detected (table S2).

Genome assembly and annotation

De novo assembly produced a high-quality chromosome-level reference genome of a female N. nebulosa (Fig. 1B), comprising 65 contigs with high contiguity of N50 = 122 megabytes (MB), which were scaffolded into 19 chromosomes using Hi-C data (fig. S1 and table S3). This new reference genome has a length of 2.43 gigabytes and contains 20,258 annotated protein-coding genes. The completeness of the assembly was assessed using BUSCO, with 8871 (96.1%) complete genes of the total of 9226 mammalian conserved orthologues. A total of 786 megabytes (32.03%) of the genome is made up of repetitive elements. The gene function annotations with the nonredundant and Swiss-Prot databases are 99.7 and 94.87%, respectively (table S4). The results of genome comparison between the mainland clouded leopard (MCL) and the domestic cat, Felis catus (felCat 9.0), involving the chromosomal variation in gas chromatography content, gene density, repeat sequences, and genomic synteny, are depicted in Fig. 1B and fig. S2.

Divergence time of Neofelis

We aligned the genome of *N. nebulosa* with three *Panthera* species (tiger, leopard, and lion) and a domestic cat as the outgroup. The aligned whole-genome sequences without repeat sequences were used to estimate divergence times. Our results indicate the divergence between Neofelis and Panthera occurred approximately 6.19 million years (Ma) ago in the Late Miocene with wide 95% confidence intervals (CIs) of 4.05 to 8.95 Ma, which is comparable to earlier estimates (6, 15). N. diardi diverged from N. nebulosa around 2.22 Ma ago (CI, 1.39 to 3.27 Ma) (Fig. 1C). The oldest fossil record of a diagnosable Panthera ancestor was found in the Tibetan Himalaya from Late Miocene–Early Pliocene (16) deposits, at a time when the global climate became cooler and more arid, causing grasslands to expand (17–19). The rapid expansion of grasslands dominated by C4 plants between 8.5 and 6.0 Ma promoted the diversification of herbivore populations (20, 21), which led to the

evolution of large mammalian carnivores, such as Panthera, which occupied the open grassland for more abundant food sources (16, 22). However, the clouded leopards' highly arboreal adaptations have limited their distribution to tropical forests (23), which is consistent with the limited fossil record (7, 24). The estimated divergence between Neofelis species (1.39 to 3.27 Ma) agrees with the previous estimates based on both nuclear and mitochondrial datasets (1, 15) but challenges a recent study (25). The earliest clouded leopard fossils are reported from late the Pleistocene and Holocene (3) of Southeast Asia and Central China (26). Glacial movements during the early Pleistocene (2.6 to 2.0 Ma) led to great changes in Southeast Asia's climate. As the rainforests contracted, they were replaced by savannas (27, 28), while humid tropical forests were limited to a few areas (29). The ancestor of clouded leopards likely occupied tropical forests in the south and north as natural refuges (30), which may have promoted genetic isolation and divergence. Subsequent sea level rises in interglacial periods erased former land bridges connecting the Sunda archipelago from the Peninsular Malaysia and contributed to further isolation of the two clouded leopard species.

Genome-wide introgression analyses

To study the correlation of local genomic phylogeny within extant Pantherinae, we constructed the topologies of locally aligned fragments across the whole genomes of two clouded leopards and three Panthera species (Fig. 1D). Our results found less than 5% phylogenetic discordance, which was sporadically scattered along the whole reference genome architecture (Fig. 1D and fig. S3), i.e., the two most frequent nonspecies tree topologies are shown as topology 2 and topology 3 in Fig. 1D. To distinguish the effects caused by introgression or ILS, which are the main causes of discordance between gene trees and species trees, we applied the software Dsuite to test presumptive introgression between Neofelis and Panthera species. The results provided values less than 0.015 and nonsignificant P values (>0.05) and Z scores (<2) (Fig. 1E). Furthermore, by dating the trees with genealogical discordant topologies, our results supported the estimated divergence time between Neofelis and Panthera species as being older than the earliest divergence time for the differentiation of Panthera species (Fig. 1F), indicating that ILS is the major contributor to the observed phylogenetic discordance. Previous studies have shown frequent postspeciation hybridization in Panthera and even strong signals of ancient introgression among different clades of the Felidae (31). Our phylogenomic results indicate strong genetic isolation of clouded leopards from tiger, lion, and leopard, which we attribute to the highly specialized arboreal niche differentiation in the former (32).

Forest adaptation in clouded leopard genome

Comparing MCL with tiger, leopard, lion, and two small cats [domestic cat and Asian leopard cat (Prionailurus bengalensis)], we identified 19,721 orthologous genes shared by all six taxa. The results of gene family alteration show that 44 gene families (176 genes) were expanded uniquely in MCL, and the expanded genes are functionally enriched into cellular process, metabolic process, immune system process, etc. (Fig. 1C, fig. S4, and table S5).

To identify specific signatures of natural selection in the clouded leopard lineage, we performed positive selection tests (see Materials and Methods) on 11,833 single-copy orthologues shared between *Neofelis* and *Panthera*. Our results revealed 153 positively selected genes (PSGs), 386 rapidly evolving genes (REGs), and 21 evolutionarily convergent genes that are strongly associated with tooth development (5 genes), pigmentation (17 genes), muscle development (5 genes), stature (4 genes), and olfaction, among others (Fig. 2A and tables S6 to S8). We highlight some of these below.

Proportionally longest canine teeth in modern cats

Clouded leopards have the longest upper canines (in relation to body size) of all living cat species. In contrast to the suffocating throat bite commonly used by other big cats to kill larger prey relative to their body size (33), clouded leopards only use a nape bite to kill larger prey, such as primates, deer, and Eurasian wild pigs (32).

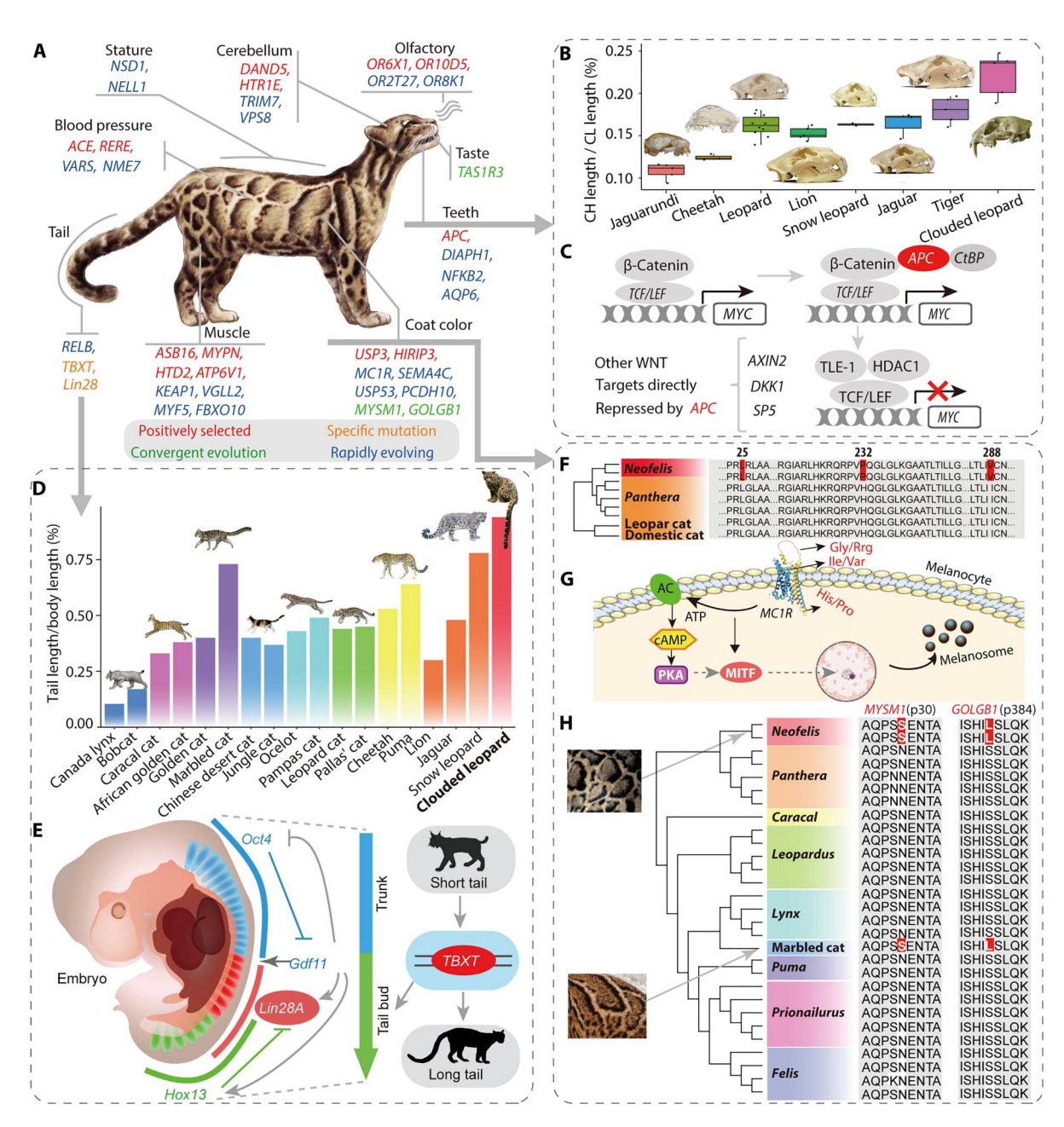


Fig. 2. Genomic signatures of arboreal adaptation in *Neofelis*. (A) Genes with signatures of adaptive evolution in *Neofelis*. (B) Clouded leopards have the largest ratio of upper canine tooth (CH) length to condylobasal-skull (CL) length among extant modern cats. (C) The positively selected *APC* gene is important in regulating tooth development in the model of the WNT–APC–β-catenin pathway. (D) Clouded leopards have the highest ratio of tail length to head-and-body length among extant modern cats. (E) The schematic shows the crucial genes associated with the trunk (*Oct4* and *Gdf11*) and tail bud (*Gdf11*, *Lin28*, *Hox13*, and *TBXT*) in embryos, and the specific mutated genes of *Lin28* and *TBXT* may affect the development of the long tail of clouded leopards compared with most other modern cats. (F and G) Location of amino acid replacements in *MC1R* influences the regulation of the formation of melanosomes in melanocyte cells. ATP, adenosine 5′-triphosphate; cAMP, adenosine 3′,5′-monophosphate; PKA, protein kinase A; MITF, microphthalmia-associated transcription factor. (H) Convergent evolution of genes *MYSM1* and *GOLGB1* associated with pigmentation formation in clouded leopards and the marbled cat.

We collected data on relative length of the canine crown height to condylobasal-skull length for extant cat species, which showed that clouded leopards have relatively the longest upper canines (Fig. 2B and table S9). One PSG and four REGs were identified in the ancestor of Neofelis (Fig. 2A and fig. S5). APC (APC regulator of WNT signaling pathway) is a crucial gene that regulates cell proliferation by down-regulating the transcription of β -catenin, a major intracellular signal transducer in the WNT signaling pathway (Fig. 2C). Mutations of APC cause dental anomalies in number and size, particularly supernumerary teeth (34), which are positively correlated with macrodontia (35).

Longest tail among modern cats

Clouded leopards process the highest ratio of tail length to headand-body length in all Felidae species (Fig. 2D and table S10). After compiling a list of 31 genes previously reported as being associated with variation in tail development (36), we detected several unique amino acid mutations in the Lin28 and TBXT genes of clouded leopards. These sequences are extremely conserved within all other modern extant cats and even other mammalian lineages (Fig. 2E and figs. S5 and S6). For LIN28A gene, one missense nucleotide mutation, which is the only amino acid variant within the LIN28A protein found across Felidae, alters the methionine at position 123 to valine (fig. S6). LIN28A has been suggested to play a crucial function in controlling the activity of tail bud axial progenitors (36). Knockout of the LIN28A gene influences the ratio of tail length to head-and-body length ratio in experiments on mice (37). In addition, compared with the two conserved RNA polymerase binding elements (CAAT) in the promoter regions of the LIN28A gene in other cats, we observed a third CAAT element in clouded leopards (fig. S7), which may influence the expression of LIN28A. In clouded leopards, the TBXT gene contains an amino acid substitution from glycine to aspartate at position 251 within the sixth exon, which was predicted to produce a significant change in charge that might alter protein function by SIFT (affecting protein function with a significant score of 0.01) and PolyPhen-2 (probably damaging with a significant score of 0.980), respectively. TBXT plays an important function in the maintenance of axial skeleton extension (38), and deletions of the sixth exon of TBXT deletion produce tailless or short-tailed phenotypes in mice (39).

Coat color and pattern

Unlike the spotted, striped, or uniform fur coloration of Panthera species, clouded leopards have a darker pelage dominated by cloudlike markings, which are an adaptation for camouflage (disruptive coloration) in dappled light in dense forests (7). Among 171 pigmentation-associated genes (40), 3 PSGs and 12 REGs were identified on the branch of the Neofelis ancestor (table S8). MC1R is a key receptor anchored on the membrane of melanocytes, which triggers melanosome production and sustains pigment synthesis to determine darker pigmentation, such as black or brown, which could contribute to effective camouflage (Fig. 2, F and G) (41). In clouded leopards, the gene for this protein (MC1R) has rapidly evolved; an amino acid substitution at position 232 from His (H; charged) to Pro (P; nonpolar) in the conservative domain of "G protein—coupled receptors family 1 profile" is estimated to probably cause a change to the charge of the protein and could potentially affect its protein function as predicted by SIFT with a score of 0.02 (<0.05 as deleterious).

Clouded leopards and the marbled cat (Pardofelis marmorata) represent an example of notable ecomorphological convergence within the Felidae, sharing similar clouded markings, proportionately long tails, and flexible ankle joints to hunt similar prey as part of a highly arboreal lifestyle (42). These similarities led previous authorities to misclassify the marbled cat within the Pantherinae lineage (43), although current genomic studies indicate the ancestor of the two lineages diverged around 12 to 15 Ma ago. We conducted screens for convergent molecular evolution between clouded leopards and the marbled cat and identified two parallel amino acid substitutions: N30S in MYSM1 gene and S384L in GOLGB1 (Fig. 2H and table S11). Previous studies showed that variants in the MYSM1 gene were closely associated with skin phenotypes (44), including abnormal hair follicle patterning or pigmentation in mouse experiments (44). Mutations in GOLGB1 have been reported to affect the formation of feather pigments (45).

Reproductive decline

One of the major challenges to ex situ conservation of clouded leopards is poor reproductive success in captivity. This has been attributed in part to a high proportion (82%) of structurally abnormal spermatozoa, the highest of all assayed felids (Fig. 3A) (46). Defects include high rates of acrosomal defects (61.60% of MCL and 50% of SCL) as well as a variety of midpiece and flagellum abnormalities (Fig. 3B) (46).

After analyzing the resequencing data of 20 MCLs, we identified 407 single-nucleotide variants in 289 protein-coding genes that were classified as highly deleterious mutations, which may cause structural and/or functional changes to the protein. We have calculated the frequencies of the highly deleterious mutations in all clouded leopard individuals in our study. The results showed that the rare variants comprised more than 31.45% (fig. S8) of all detected deleterious mutations in the sample of clouded leopards. We further scanned the population genomic data of different Panthera species. The results of these tests showed that the deleterious mutations found in our sample of the MCLs occurred at lower levels in different Panthera species (tables S12 to S15). Gene ontology (GO) analysis of these 289 genes identified significant (P < 0.05) enrichments in metabolic process (GO:0008152), response to stimulus (GO:00508996), and reproductive process (GO:0022414) (Fig. 3C, fig. S9, and tables S16 and S17). Thirty-one deleterious mutation genes (ABCA15, ACE3, etc.) have been previously reported to be associated with sperm development (table S18), including gamete generation and cilium movement, and cellular processes involved in reproduction in multicellular organisms, which can cause the diseases of varicocele and male infertility (Fig. 3D).

Major histocompatibility complex (MHC) genes play important roles in the immune response, and several studies have identified associations with vertebrate reproduction (47). In comparison to the MHC gene region of the domestic cat (3.17 megabytes) (48), we found that clouded leopards had the shortest region length (2.69 megabytes) and the fewest classical Feline Leukocyte Antigen (FLA) gene numbers among all Pantherinae species (Fig. 3E). Two lost FLA genes in clouded leopards, including FLA-G and partial of FLA-M, are homologous to human HLA Class I Histocompatibility Antigen, B Alpha Chain (HLA-B) and HLA Class I Histocompatibility Antigen, C Alpha Chain (HLA-C) gene (48), genetic variants of which have been associated with human male infertility (49).

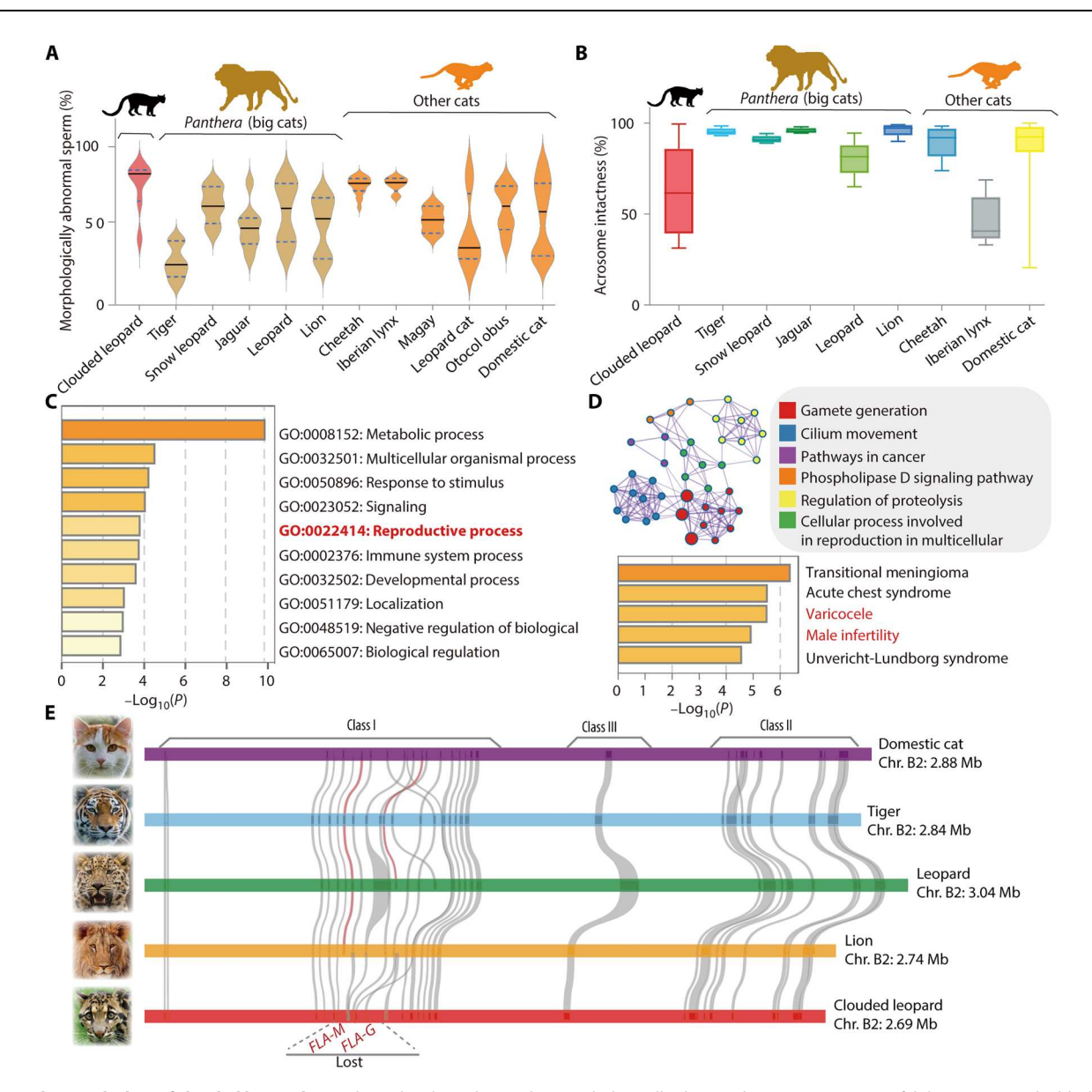


Fig. 3. Reproductive decline of clouded leopards. (A) The violin plot indicates the morphologically abnormal sperm rate in extant felid species (46). The black solid line on each violin plot represents the median value, and the blue dashed lines represent the top or bottom quartiles. (B) Box plots of acrosome intactness. The y axis represents the proportion of acrosome intactness (46). The colored box plots represent felid species along the x axis. (C) Metascape bar graph showing the top-level GO biological processes of the 289 highly deleterious mutated genes. (D) Metascape network enrichment analysis (top) and the enrichment analysis in DisGeNET (bottom) of 31 reproduction genes. (E) Gene organization in the MHC gene clusters of five felids. The colored boxes indicate three different classes of MHC genes (class I, class III, and class II) with the arrangement in order along the chromosomes. The red colinear curves indicate the genes (FLA-G and FLA-M) that were lost in clouded leopard.

Genetic diversity in clouded leopards

We compared the average heterozygosity of clouded leopards to estimates for other cat species. The heterozygosity of the MCL (0.0406%) is similar to that of the African cheetah, *Acinonyx jubatus*, and about two- to fivefold lower than most *Panthera* species (Fig. 4A), with the exception of the snow leopard, *Panthera uncia* (0.0430%). Heterozygosity of the SCL (0.0154%) is the lowest of all Pantherinae species and similar to that of the Iberian lynx (*Lynx pardinus*) (0.0102%), which is considered the most endangered extant felid (Fig. 4B and table S19) (13). Previous studies have illustrated the effects of inbreeding on genetic diversity of

endangered species (50). Here, we evaluated the inbreeding coefficient by runs of homozygosity (ROHs) and found very high genomic inbreeding coefficients in MCLs ($F_{\rm ROH} = 34.72\%$) and SCLs ($F_{\rm ROH} = 52.02\%$), with values greater than that of the Iberian lynx ($F_{\rm ROH} = 32\%$) (Fig. 4C, fig. S10, and table S20) (13).

To further understand the historical background of genetic erosion in clouded leopards, we investigated the demographic history of each species with the pairwise sequentially Markovian coalescent (PSMC) approach. The results indicated a continuous decline of effective population size (*Ne*) of *Neofelis* in the past 1 million years (Fig. 4D and fig. S11). Extremely low genomic

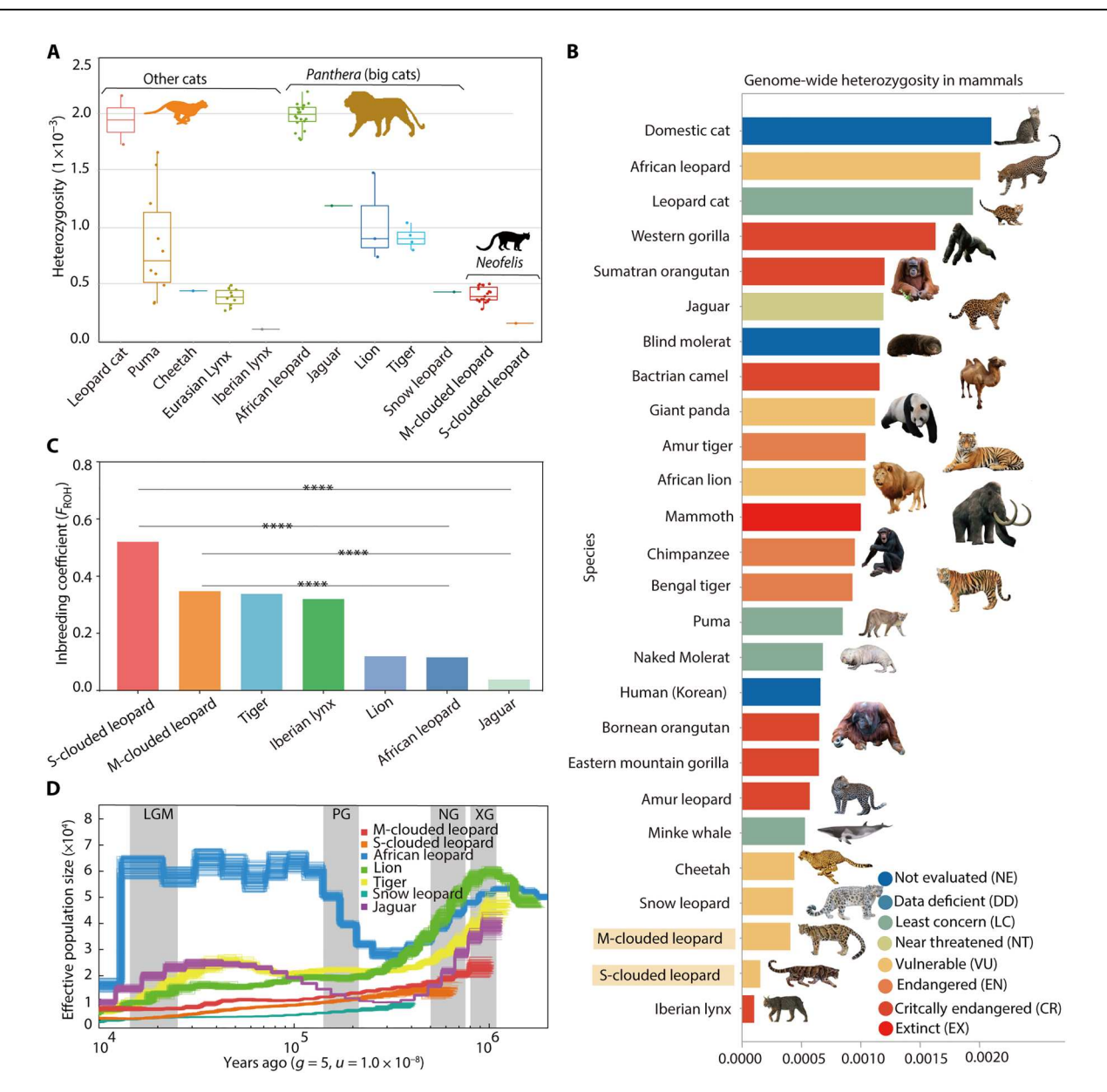


Fig. 4. Loss of genetic diversity and elevated inbreeding in clouded leopards. (**A**) Average heterozygosity of different felids. (**B**) The level of genome-wide heterozygosity of the two clouded leopards in comparison to other mammals (the image source listed in table S26), in relation to conservation status (IUCN Red List of Threatened Species). (**C**) Comparison of inbreeding coefficients (F_{ROH}) of two clouded leopards and other living felids. *****P < 0.001 (**D**) The estimated historical changes in effective population sizes (Ne) of Pantherinae species using PSMC. The gray-shaded boxes represent the Xixiabangma Glaciation (XG), Naynayxungla Glaciation (NG), the second Pleistocene Glacial Period (PG), and the last glacial maximum (LGM).

heterozygosity, as well the severity of inbreeding in each clouded leopard species, highlights the need for urgent conservation efforts for both species.

Population genetics and genome-wide selective sweep test

We first investigated the population structure of 20 MCLs by estimating a neighbor-joining (NJ) tree based on 4.16 million autosomal SNPs. The tree divided MCLs into two groups (Fig. 5A) also supported by principal components analysis (PCA) (Fig. 5B). We further estimated per-individual ancestry proportions using software ADMIXTURE (51). The results supported the model with a best fit to the dataset as two ancestral source populations (K = 2)

(Fig. 5C). We scanned the genome for regions with extreme divergence in allele frequency ($F_{\rm ST}$) and the highest differences in genetic diversity (π log ratio) in 50-kb sliding windows on autosomes (Fig. 5D). In total, we identified 115 candidate regions covering 99 genes ($ZF_{\rm ST} > 3.09$, π log ratio > 1.778) both with a significance level of P < 0.001 (fig. S12 and tables S21 and S22). To determine whether similar gene functions were under selection in the entire gene network, we performed an enrichment analysis using KOBAS (table S23). We found the identified candidate genes under selection to be overrepresented (corrected P < 0.05) in pathways related to high-altitude adaptation, including circadian entrainment, galactose metabolism, hypoxia-inducible factor 1

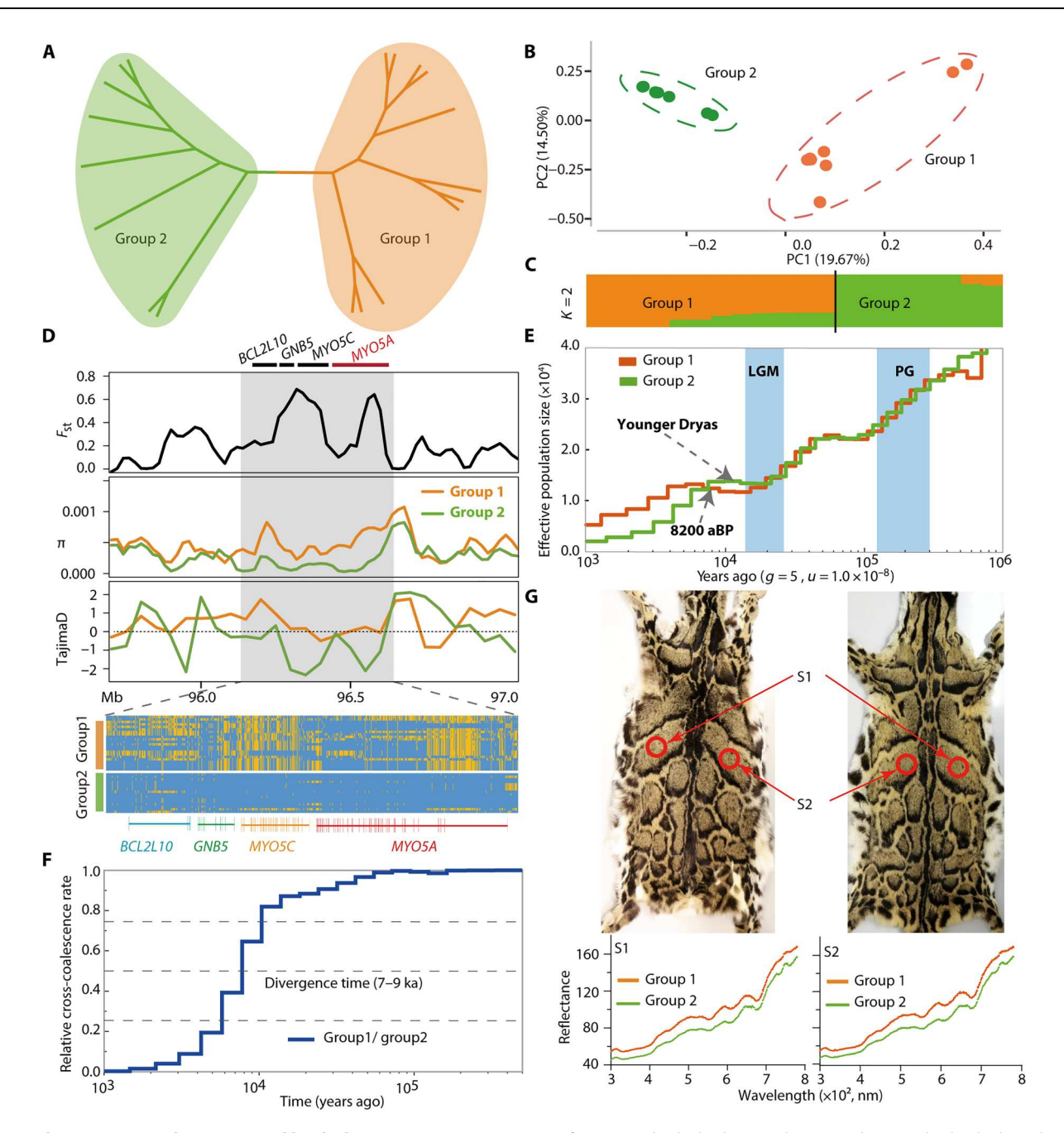


Fig. 5. Population structure, divergence, and local adaptation in MCLs. (**A**) NJ tree of 20 MCL individuals, showing divergence between lowland-adapted (red) and high altitude–adapted (orange) MCLs. (**B**) The PCA for 20 MCL individuals. (**C**) Population structure of 20 MCLs inferred from ADMIXTURE with K = 2. (**D**) A region with significant genetic divergence ($F_{ST} = 4.793$ and π ratio = 2.652) between the two MCL populations contains four genes: *GNB5*, *BCL2L10*, *MYO5C*, and *MYO5A*. The haplotypes were hierarchically clustered within each MCL group. The major allele at each SNP position in group1 (allele frequency ≥ 50%) is shown in yellow and the minor allele in blue. (**E**) Demographic history of two MCL populations inferred from MSMC. The blue-shaded boxes represent the ice ages described in Fig. 4D. (**F**) Inferred relative cross-coalescence rates between two MCL populations. (**G**) Two obvious regions of clouded leopard pelages from S1 to S2 were used to detect reflectance along the different wavelengths.

(HIF-1) signaling pathway, starch and sucrose metabolism, and fructose and mannose metabolism. In addition, some of the significant GO terms (corrected P <0.05) were the glucose 6-phosphate metabolic process and the glycolytic process. These pathways related to high-altitude adaptation and GO terms involved three genes (HK1, HKDC1, and CAMK2G). HK1 plays an important

role in the cardioprotective mechanism induced by adaptation to severe intermittent hypobaric hypoxia (52).

In addition, we detected a candidate region covering the *BCL2L10*, *GNB5*, *MYO5C*, and *MYO5A* genes, which showed a significant local reduction in nucleotide diversity (Fig. 5D). MYO5A encodes myosin VA, which is an intracellular organelle transport

protein with important functions in the dendritic spines of melanocytes (53). Previous study has reported MYO5A variants associated with coat color dilution (54). Compared with animals in humid and warm environments, animals in dry and cold areas display lighter coat colors, which may be a plastic response to different climates (55). Studies have found that GNB5 plays crucial roles in parasympathetic regulation of heart rate (56), and mutations or knockout experiments of GNB5 were correlated with significant changes in heart rate (57). The microdeletions in GNB5, BCL2L10, and MYO5C were found to be linked to cardiac arrhythmias (58). A multiple sequentially Markovian coalescent (MSMC) plot showed that clouded leopards went through a constant population decline (Fig. 5E), and MSMC plot indicated these genetic differences between the two subpopulations of MCLs occurred between 7 and 9 ka (Fig. 5F), probably associated with the largest amplitude of a cooling event at 8200 BP in the Holocene (59).

To verify differences in coat color, we recorded reflectance of two groups of clouded leopards' pelages in a museum collection, from which two obvious areas of S1 and S2 were used to detect reflectance (Fig. 5G and fig. S13). Considering that most mammals can see light with a wavelength range of 380 to 780 nm (400 to 700 on primates) (60), we plotted the distributions of pelage reflectance values along the wavelength range of visible light in mammals (Fig. 5G and table S24). From the comparison, group 1 MCLs showed higher reflectance at all selected spots (S1-S2) compared with group 2 at the same wavelengths; paired t tests show that two groups both at S1 with a mean difference of 12.00 (95% CI, 11.79 to 12.21) and at S2 with a mean difference of 12.14 (95% CI, 11.85 to 12.43) are significantly different (P < 0.05) (Fig. 5G).

These data would appear to support the differentiation of the MCL into two subspecies that were previously recognized (24), N. n. nebulosa from China and Southeast Asia and N. n. macrosceloides, which ranges from northern Myanmar to Nepal and India, including at higher elevations. However, there are no distinctive morphological differences between these two putative subspecies (2), and it is likely that this recent physiological differentiation represents different ecotypes rather than subspecies. Moreover, the high-altitude adaptations occur in clouded leopards whose ancestors originated from Vietnam, which is outside the distribution of putative *N. n. macrosceloides*. These two ecotypes should probably be managed separately in both in situ and ex situ conservation.

We identified genetic adaptions using comparative genomic approaches that play potentially play crucial roles in the clouded leopards' high dependence on arboreal habitats. Our study has identified low levels of heterozygosity and high levels of inbreeding as serious concerns faced by remnant populations of clouded leopards. Our results support a probable causal association between ancient Ice Age-induced climate changes that precipitated a continuous historical decline of the effective population sizes of the two species of clouded leopards, which continues to deteriorate due to the modern illegal wildlife trade and deforestation. Severe habitat fragmentation has probably accelerated the accumulation of deleterious mutations due to high levels of inbreeding. High levels of inbreeding and deleterious genes are key indicators of the genetic crisis affecting clouded leopard conservation and highlight the need for urgent action for the survival of these imperiled big cat species. Our study on the population genetics and adaptive evolution of the clouded leopards enables a comprehensive understanding of the genetic basis of the key adaptations of these big cats.

Knowledge of the genetic structure, adaptive potential, and evolutionary dynamics of populations of both clouded leopards will facilitate the development of conservation programs that target the maintenance of genetic diversity in the wild and captivity, planning for protected areas and improving captive breeding to help the conservation and restoration of clouded leopards.

MATERIALS AND METHODS

Genome sequencing, assembly, and annotation

We sampled 20 MCLs (N. nebulosa) and one SCL (N. diardi) from specimens in zoos and museums (table S1) based on DNA extracted from blood. High-quality genomic DNA were extracted from clouded leopards' blood using DNeasy Blood and Tissue Kit DNA kit (QIAGEN, Hilden, Germany) and delivered to the GrandOmics company (Wuhan, China) for library preparation and sequencing. One paired-end library $[2 \times 150 \text{ base pairs (bp)}]$ with insertion sizes of 350 bp was constructed with VAHTS Universal DNA Library Prep Kit for Illumina V2 kit (Vazyme, Nanning, China) and sequenced on the Illumina NovaSeq 6000 platform. The DNA molecule of approximately 20 kb was selected by the PippinHT system (Sage Science, USA) for long-read sequencing; further, Nanopore library was constructed using the Genomic DNA by Ligation (SQK-LSK109, Oxford Nanopore Technology, UK) and sequenced three flow cells on Nanopore PromethION sequencer instrument (Oxford Nanopore Promethion sequencer instrument (Oxford Nanopore Technologies, UK). All long-read Nanopore sequences were aligned against themselves to generate consensus sequences using NEXTDENOVO v2.4.0 (https://github.com/Nextomics/NextDenovo) with default settings. After self-correction and trimming, the corrected long reads were used for genome assembly using FLYE v2.8.1-b1676 (61) with parameters "--nano-raw --iterations 2." Contigs were further polished by NEXTDOLIGIA at 2.1 (62). These recently a familiar page 2. by NEXTPOLISH v1.3.1 (62). Three rounds of polish were performed using Nanopore reads and Illumina paired-end short reads. All options within the NEXTPOLISH configuration file were set to their default settings, except for the modification of "lgs_minimap2_options" to "-x map-ont." Redundant sequences were identified and removed with PURGE_DUPS v1.2.5 (63). To obtain a chromosome-level assembly, the assembled contigs were anchored by Hi-C reads applying Juicer v1.5.7 (64) and 3D-DNA v180922 (65). Juicebox Assembly Tools v1.9.9 (66) was then used for manual curation to detect and correct misjoins and to improve assembly quality. Last, Benchmarking Universal Single-Copy Orthologs v4.1.2 (BUSCO, http://busco.ezlab.org) was used to evaluate the completeness of the gene sets in our draft genome with parameters "-m genome -l mammalia_odb10."

Repeatmasker v4.0.7 (www.repeatmasker.org) was used to identify repeats on the basis of the homology predictions with the Repbase database v2017-01-27 of known repeats in Carnivora. RepeatModeler v1.0.11 (http://repeatmasker.org/RepeatModeler/) was applied to construct the de novo repeat custom library, which were used to predict repeats by RepeatMasker.

Homology and de novo predictions were carried out to identify the structures of protein-coding genes using the following approaches. First, orthologous protein-coding evidence from homologous species (tiger, lion, leopard, domestic cat, puma, dog, and human) was downloaded from National Center for Biotechnology Information (NCBI) and independently used to predict the proteincoding genes of clouded leopard using the GeMoMa pipeline v1.6.1

(67). The predicted gene sets were then combined with the module GAF from GeMoMa using the filter "iAA>=0.8 and ce/rce==1." Second, downloaded orthologous protein sets were aligned to the clouded leopard genome using TBLASTN v2.11.0 with an e value parameter of 1×10^{-5} , and the aligned best Hits regions were further used for gene prediction with GeneWise v2-4-1 (68) programme. Third, the prior predicted genes from GeMoMa and GeneWise were used as training-gene sets to perform the de novo predictions by Augustus v3.3.1 (69), GlimmerHMM v3.0.4 (70), and SNAP v2017-03-01 (71). Last, the predicted gene structures from both homology and de novo predictions were combined on the basis of a weighted consensus by EVidenceModeler v 1.1.1 (https://github.com/EVidenceModeler/EVidenceModeler).

Phylogenomic analysis and divergence time estimation

We aligned three Panthera genomes and two Neofelis genomes to the reference genome of the domestic cat (felCat 9.0) using LAST v1133 (72) with parameters "-m100, -E0.05," and MULTIZ v11.2 (73) to combine all pairwise alignments into a six-species wholegenome alignment data (table S25). For the phylogeny of local alignments of sliding windows among all compared genomes, we partitioned the data into nonoverlapping sliding windows with varying window sizes of 20, 50, 100, and 200 kb to reconstruct phylogenetic trees. All windows with more than 75% gaps were removed. RAxML v 8.2.12 (74) was used to construct maximum likelihood trees from each alignment, and the low consensus trees (bootstrap < 50%) were discarded.

Sequences from windows with identical tree topologies were concatenated into supermatrices (83.92 megabytes) using inhouse made Perl script and independently used for the divergence time estimation using MCMCTree in PAML v4.5 (75), which was applied to calculate the divergence time with two previously used time calibrations: (i) The crown radiation of extant felids from 11.46 to 16.35 Ma ago (15) and (ii) the crown radiation of Panthera with a minimum of 3.8 Ma.

Orthologue identification

Protein-coding genes from five felid species (*F. catus*, *P. bengalensis*, Panthera tigris, Panthera leo, and Panthera pardus) were downloaded from NCBI and Ensembl databases (table S25), and the longest transcript of each gene was selected to identify orthologous groups of genes for the two clouded leopard species using the Orthofinder pipeline v2.5.2 (https://github.com/davidemms/OrthoFinder), producing a total of 11,833 single-copy orthologous genes. The singlecopy gene datasets were then aligned using Prank v170427 (76). RAxml v8.2.12 (74) with a PROTGAMMAWAG model was applied to reconstruct a phylogenetic tree for each protein sequence of gene. With the classified orthologous genes and the estimated time tree, we performed a CAFÉ v4.2 (77) analysis to detect the gene family expansions and contractions, in which the default parameters of lambda (-s) and a P value cutoff of 0.05 were used to detect the significant expansions/contractions along each branches.

Adaptation analysis

Nonsynonymous and synonymous substitution rates (Ka/Ks) were calculated using codeml program in PAML v4.5 (75) package. We used the branch site model and two-ratio models to detect signatures of natural selection on coding genes of Neofelis. Statistical significance was determined using likelihood ratio tests. The candidate

genes were further functionally annotated and tested for gene enrichment into the GO items and Kyoto Encyclopedia of Genes and Genomes (KEGG) pathways by Metascape (78). To investigate the effects of the mutations on their functions and protein structures, we applied the bioinformatic tools PolyPhen-2 (http:// genetics.bwh.harvard.edu/pph2/) (the prediction as probably damaging, possibly damaging or benign), SIFT (https://sift.bii.a-star. edu.sg/) (amino acids with the scores of <0.05 are predicted to be deleterious) and SWISS-MODEL (https://swissmodel.expasy.org) to assess the influences of amino acid substitutions.

Read alignment and variant calling

We used the Burrows-Wheeler Aligner (BWA mem, v0.7.17-r1188) (79) to align the high-quality Illumina short reads to the reference assembly of MCL with default parameters. SAMtools and Picard Tools Version 1.56 (http://broadinstitute.github.io/picard) were used to sort bam files and filter duplicate reads. Last, SNPs calling within all genomic alignments were performed using the command HaplotypeCaller and GenotypeGVCFs of the Genome Analysis ToolKit package v3.8 (80) and then were filtered using the Variant-Filtration command with the following criteria: "DP < 161; DP > 1453; QD < 2.0; FS > 60.0; MQ < 40.0; MQRankSum < -12.5; Read-PosRankSum < -8.0; SOR > 3.0." High-quality SNPs were exported into variant call format (VCF) files for further population genetics tests.

Introgression tests

We performed ABBA/BABA four-taxon D statistic tests using Dsuite v0.4-r43 (81) to evaluate introgression between clouded leopards and Panthera species, including of the trios: (MCL, (leopard, lion)), domestic cat), ((MCL, (tiger, lion)), domestic cat), as well as the SCL. Specifically, we adopt the "Dtrios" progress of Dsuite to assess historical

ically, we adopt the "Dtrios" progress of Dsuite to assess historical 3 gene flow using the generated VCF files. To assess whether *D* values calculated with Dsuite were significantly larger than zero, a standard block jackknife procedure (82) was used to calculate the Z scores with a cutoff of 2 and the associated P values with a cutoff of 0.05 as the significant ones.

Identification of deleterious mutations

First, the annotation of clouded leopard genome in GTF format was used to construct the local database by SnpEff v5.0 (http://snpeff. sourceforge.net/), and the earlier generated VCF files of 20 resequenced MCLs were used as the input data to evaluate the potential effects of genetic variants. The mutations ranked as "high" functional effects were considered deleterious mutations used in further gene enrichment tests.

ROHs and genome-wide heterozygosity

We identified ROHs using Plink v1.9 (83) with the following parameters: --homozyg -homozyg-window-snp 20 --homozygwindow-het 2 -homozyg-density 50 -homozyg-kb 50. The genomic inbreeding coefficient (F_{ROH}) refers to the ratio of the total length of ROH to the whole genome. The evaluation of genome-wide heterozygosity was calculated by the proportion of heterozygous sites in the genome using Plink with the parameter "--het."

Demographic history

PSMC v0.6.5-r67 (84) method was used to assess changes in effective population size (Ne) of the MCLs over time, relative to tigers, lions, and other Felidae. We selected individuals with a high sequencing depth to ensure the quality of the consensus sequence. Parameters were set as -N25, t15, -r5, -p '4 + 25*2 + 4 + 6'. Here, we assumed that the mutation rate of the MCL as 1 × 10⁻⁸ and the generation time as 5 years (31). MSMC2 v2.1.1 (85) was used to infer population separation history. To obtain a greater resolution, we estimated divergence time between the two clouded leopard subgroups using eight haplotypes per group and then used key model "1*2 + 25*1 + 1*2" to estimate the differentiation time, mutation rate as 1×10^{-8} and the generation time as 5 years (31).

Population structure

We performed PCA of all individuals using the smart PCA programme in EIGENSOFT v5.0 (www.hsph.harvard.edu/alkesprice/software/). The significance level of the eigenvectors was determined by the Tracy-Widom test. Genome-wide admixtures among the MCL population were quantified using ADMIXTURE v1.3.0 (51), which was run for each possible group number (Kfrom 2 to 4) with 1000 bootstrap replicates. We calculated a distance matrix (1-IBS) based on all samples in Plink (version 1.9) (83). We further used MEGA v11 (86) to construct an NJ tree based on the genetic distance matrix and performed 1000 bootstrap replicates to assess nodal support. Last, we used PopLDdecay (87) to evaluate linkage disequilibrium patterns. Natural selection typically results in lower genetic diversity within populations and higher genetic differentiation between populations. F_{ST} (genetic differentiation index) is a standardized measure of the variance of allele frequencies between populations. Here, we used VCFtools v0.1.16 (http:// vcftools.sourceforge.net) to calculate F_{ST} between the two populations and the nucleotide diversity π within the population. F_{ST} was calculated with parameters as follows: "--weir-fst-pop group1 --weir-fst-pop group2 --fst-window-size 50,000 --fst-window-step 20,000 --maf 0.05 --max-missing 0.90." Nucleotide diversity π was calculated with parameters as follows: "--window-pi 50,000 --window-pi-step 20,000 --maf 0.05 --max-missing 0.90." We lastly used KOBAS (http://bioinfo.org/kobas) to perform KEGG pathway and GO term enrichment analyses for selected genes located in specific regions.

Diffuse reflectance spectroscopy

Data acquisition from Maya spectrometers with an optical fiber probe (Ocean Optics, QR400-7-SR) was controlled by oceanview v2.0.8. Measurements were made directly on the images of the two groups of clouded leopard pelages in the collection of National Museums Scotland; muscle samples from these same specimens were used to generate whole-genome sequences reported here. The reflectance of each scanned region of each pelage was recorded three times, and the mean value was recorded. GraphPad Prism v9.0.0 was used to depict the reflectance distributions along the wavelengths, and significant tests were carried out on paired t test.

Ethics statement

The study protocols received ethical approval from the Ethics Committee of the Guangzhou Zoo (permit number: GZZ2020C03, 18 April 2020), National Museum Scotland (GB003), and the Kunming Institute of Zoology (CN005) under the UK CITES

label 1887. The study adhered to good clinical practice guidelines and complied with relevant local regulations. All research procedures were conducted in full compliance with national and institutional regulations.

Supplementary Materials

This PDF file includes:

Figs. S1 to S13 Legends for tables S1 to S26 References

Other Supplementary Material for this manuscript includes the following: Tables S1 to S26

REFERENCES AND NOTES

- V. A. Buckley-Beason, W. E. Johnson, W. G. Nash, R. Stanyon, J. C. Menninger, C. A. Driscoll, J. Howard, M. Bush, J. E. Page, M. E. Roelke, G. Stone, P. P. Martelli, C. Wen, L. Ling, R. K. Duraisingam, P. V. Lam, S. J. O'Brien, Molecular evidence for species-level distinctions in clouded leopards. *Curr. Biol.* 16, 2371–2376 (2006).
- A. C. Kitchener, M. A. Beaumont, D. Richardson, Geographical variation in the clouded leopard, Neofelis nebulosa, reveals two species. Curr. Biol. 16, 2377–2383 (2006).
- H. Hemmer, Untersuchungen zur stammesgeschichte der pantherkatzen (Pantherinae).
 Teil II: Studien zur ethologie des nebelparders Neofelis nebulosa (Griffith 1821) und des Irbis Uncia uncia (Schreber 1775). Veröff. Zool. Staatssammlung München 12, 155–247 (1968).
- 4. P. Christiansen, J. S. Adolfssen, Bite forces, canine strength and skull allometry in carnivores (Mammalia, Carnivora). *J. Zool.* **266**, 133–151 (2005).
- M. Antón, À. Galobart, Neck function and predatory behavior in the scimitar toothed cat Homotherium latidens (Owen). J. Vertebr. Paleontol. 19, 771–784 (1999).
- W. E. Johnson, E. Eizirik, J. Pecon-Slattery, W. J. Murphy, A. Antunes, E. Teeling, S. J. O'Brien, The late Miocene radiation of modern Felidae: A genetic assessment. *Science* 311, 73–77 (2006).
- L. Werdelin, N. Yamaguchi, W. E. Johnson, S. J. O'Brien, Phylogeny and evolution of cats (Felidae), in *The Biology and Conservation of Wild Felids*, D. M. Macdonald, A. Loveridge, A., eds., (Oxford Univ. Press, 2010), pp. 59–82.
- D. W. Macdonald, H. M. Bothwell, Ż. Kaszta, E. Ash, G. Bolongon, D. Burnham, Ö. E. Can, A. Campos-Arceiz, P. Channa, G. R. J. D. Clements, Distributions, multi-scale habitat modelling identifies spatial conservation priorities for mainland clouded leopards (*Neofelis nebulosa*). *Biol. Conserv.* 25, 1639–1654 (2019).
- A. Hearn, J. Ross, J. Brodie, S. Cheyne, I. Haidir, B. Loken, J. Mathai, A. Wilting, J. McCarthy, Neofelis diardi. The IUCN Red List of Threatened Species 2015. e. T136603A50664601 (2015).
- W. J. Petersen, T. Savini, D. Ngoprasert, Strongholds under siege: Range-wide deforestation and poaching threaten mainland clouded leopards (*Neofelis nebulosa*). Glob. Ecol. Conserv. 24, e01354 (2020).
- 11. C. Santiapillai, K. R. Ashby, The clouded leopard in Sumatra. Oryx 22, 44-45 (1988).
- P. Dobrynin, S. Liu, G. Tamazian, Z. Xiong, A. A. Yurchenko, K. Krasheninnikova, S. Kliver, A. Schmidt-Küntzel, K.-P. Koepfli, W. Johnson, L. F. K. Kuderna, R. García-Pérez, M. de Manuel, R. Godinez, A. Komissarov, A. Makunin, V. Brukhin, W. Qiu, L. Zhou, F. Li, J. Yi, C. Driscoll, A. Antunes, T. K. Oleksyk, E. Eizirik, P. Perelman, M. Roelke, D. Wildt, M. Diekhans, T. Marques-Bonet, L. Marker, J. Bhak, J. Wang, G. Zhang, S. J. O'Brien, Genomic legacy of the African cheetah, *Acinonyx jubatus. Genome Biol.* 16, 277 (2015).
- F. Abascal, A. Corvelo, F. Cruz, J. L. Villanueva-Cañas, A. Vlasova, M. Marcet-Houben, B. Martínez-Cruz, J. Y. Cheng, P. Prieto, V. Quesada, J. Quilez, G. Li, F. García, M. Rubio-Camarillo, L. Frias, P. Ribeca, S. Capella-Gutierrez, J. M. Rodríguez, F. Câmara, E. Lowy, L. Cozzuto, I. Erb, M. L. Tress, J. L. Rodriguez-Ales, J. Ruiz-Orera, F. Reverter, M. Casas-Marce, L. Soriano, J. R. Arango, S. Derdak, B. Galán, J. Blanc, M. Gut, B. Lorente-Galdos, M. Andrés-Nieto, C. López-Otín, A. Valencia, I. Gut, J. L. García, R. Guigó, W. J. Murphy, A. Ruiz-Herrera, T. Marques-Bonet, G. Roma, C. Notredame, T. Mailund, M. M. Albà, T. Gabaldón, T. Alioto, J. A. Godoy, Extreme genomic erosion after recurrent demographic bottlenecks in the highly endangered Iberian lynx. *Genome Biol.* 17, 251 (2016).
- D. E. Wildt, J. Howard, L. Hall, M. Bush, Reproductive physiology of the clouded leopard: I. Electroejaculates contain high proportions of pleiomorphic spermatozoa throughout the year. *Biol. Reprod.* 34, 937–947 (1986).
- G. Li, B. W. Davis, E. Eizirik, W. J. Murphy, Phylogenomic evidence for ancient hybridization in the genomes of living cats (Felidae). Genome Res. 26, 1–11 (2016).

SCIENCE ADVANCES | RESEARCH ARTICLE

- Z. J. Tseng, X. Wang, G. J. Slater, G. T. Takeuchi, Q. Li, J. Liu, G. Xie, Himalayan fossils of the oldest known pantherine establish ancient origin of big cats. *Proc. R. Soc. B. Biol. Sci.* 281, 20132686 (2014)
- T. D. Herbert, K. T. Lawrence, A. Tzanova, L. C. Peterson, R. Caballero-Gill, C. S. Kelly, Late Miocene global cooling and the rise of modern ecosystems. *Nat. Geosci.* 9, 843–847 (2016).
- C. A. Strömberg, Evolution of grasses and grassland ecosystems. Annu. Rev. Earth Planet. Sci. 39, 517–544 (2011).
- C. Hoorn, T. Ohja, J. Quade, Palynological evidence for vegetation development and climatic change in the sub-Himalayan zone (Neogene, Central Nepal). *Palaeogeogr. Palaeoclimatol. Palaeoecol.* 163, 133–161 (2000).
- A. K. Behrensmeyer, J. Quade, T. E. Cerling, J. Kappelman, I. A. Khan, P. Copeland, L. Roe, J. Hicks, P. Stubblefield, B. J. Willis, The structure and rate of late Miocene expansion of C4 plants: Evidence from lateral variation in stable isotopes in paleosols of the Siwalik Group, northern Pakistan. Geol. Soc. Am. Bull. 119, 1486–1505 (2007).
- Y. Wang, E. Kromhout, C. Zhang, Y. Xu, W. Parker, T. Deng, Z. Qiu, Stable isotopic variations in modern herbivore tooth enamel, plants and water on the Tibetan Plateau: Implications for paleoclimate and paleoelevation reconstructions. *Palaeogeogr. Palaeoclimatol. Palae-oecol.* 260, 359–374 (2008).
- J. Seidensticker, On the ecological separation between tigers and leopards. Biotropica 8, 225–235 (1976).
- A. Wilting, F. Fischer, S. Abu Bakar, K. E. Linsenmair, Clouded leopards, the secretive topcarnivore of South-East Asian rainforests: Their distribution, status and conservation needs in Sabah, Malaysia. BMC Ecol. 6, 16 (2006).
- A. C. Kitchener, C. Breitenmoser-Würsten, E. Eizirik, A. Gentry, L. Werdelin, A. Wilting, N. Yamaguchi, A. V. Abramov, P. Christiansen, C. Driscoll, A revised taxonomy of the Felidae: The final report of the Cat Classification Task Force of the IUCN Cat Specialist Group. Cat News 11, 1–80 (2017).
- M. G. Bursell, R. B. Dikow, H. V. Figueiró, O. Dudchenko, J. P. Flanagan, E. L. Aiden, B. Goossens, S. K. S. S. Nathan, W. E. Johnson, K.-P. Koepfli, P. B. Frandsen, Whole genome analysis of clouded leopard species reveals an ancient divergence and distinct demographic histories. iScience 25, 105647 (2022).
- X. Wu, W. Liu, X. Gao, G. J. C. S. B. Yin, Huanglong cave, a new late Pleistocene hominid site in Hubei Province, China. *Chinese Sci. Bull.* 51, 2493–2499 (2006).
- C. H. Cannon, R. J. Morley, A. B. Bush, The current refugial rainforests of Sundaland are unrepresentative of their biogeographic past and highly vulnerable to disturbance. *Proc. Natl. Acad. Sci. U.S.A.* 106, 11188–11193 (2009).
- 28. R. J. Morley, Origin and Evolution of Tropical Rain Forests (John Wiley & Sons, 2000).
- D. S. Woodruff, Biogeography and conservation in Southeast Asia: How 2.7 million years of repeated environmental fluctuations affect today's patterns and the future of the remaining refugial-phase biodiversity. *Biodivers. Conserv.* 19, 919–941 (2010).
- F. Gathorne-Hardy, R. Davies, P. Eggleton, D. Jones, Quaternary rainforest refugia in South-East Asia: Using termites (Isoptera) as indicators. *Biol. J. Linn. Soc.* 75, 453–466 (2002).
- 31. H. V. Figueiro, G. Li, F. J. Trindade, J. Assis, F. Pais, G. Fernandes, S. H. D. Santos, G. M. Hughes, A. Komissarov, A. Antunes, C. S. Trinca, M. R. Rodrigues, T. Linderoth, K. Bi, L. Silveira, F. C. C. Azevedo, D. Kantek, E. Ramalho, R. A. Brassaloti, P. M. S. Villela, A. L. V. Nunes, R. H. F. Teixeira, R. G. Morato, D. Loska, P. Saragueta, T. Gabaldon, E. C. Teeling, S. J. O'Brien, R. Nielsen, L. L. Coutinho, G. Oliveira, W. J. Murphy, E. Eizirik, Genome-wide signatures of complex introgression and adaptive evolution in the big cats. Sci. Adv. 3, e1700299 (2017).
- 32. M. Sunquist, F. Sunquist, Wild Cats of the World (University of Chicago Press, 2017).
- P. Christiansen, Sabertooth characters in the clouded leopard (Neofelis nebulosa Griffiths 1821). J. Morphol. 267, 1186–1198 (2006).
- F. Yu, W. Cai, B. Jiang, L. Xu, S. Liu, S. Zhao, A novel mutation of adenomatous polyposis coli (APC) gene results in the formation of supernumerary teeth. J. Cell. Mol. Med. 22, 152–162 (2018).
- A. P. Santos, M. M. Ammari, L. F. Moliterno, J. C. Júnior, First report of bilateral supernumerary teeth associated with both primary and permanent maxillary canines. *J. Oral Sci.* 51, 145–150 (2009).
- M. Mallo, The vertebrate tail: A gene playground for evolution. Cell. Mol. Life Sci. 77, 1021–1030 (2020).
- 37. L. Koch, The long and the short of it. Nat. Rev. Genet. 20, 131 (2019).
- S. Schulte-Merker, F. Van Eeden, M. E. Halpern, C. Kimmel, C. Nusslein-Volhard, No tail (ntl) is the zebrafish homologue of the mouse T (Brachyury) gene. *Development* 120, 1009–1015 (1994)
- B. Xia, W. Zhang, A. Wudzinska, E. Huang, R. Brosh, M. Pour, A. Miller, J. S. Dasen, M. T. Maurano, S. Y. Kim, The genetic basis of tail-loss evolution in humans and apes. Br. J. Dermatol., 10.1101/2021.09.14.460388 (2021).
- 40. L. L. Baxter, D. E. Watkins-Chow, W. J. Pavan, S. K. Loftus, A curated gene list for expanding the horizons of pigmentation biology. *Pigment Cell Melanoma Res.* **32**, 348–358 (2019).

- E. M. Wolf Horrell, M. C. Boulanger, J. A. D'Orazio, Melanocortin 1 receptor: Structure, function, and regulation. Front. Genet. 7, 95 (2016).
- P. Singh, D. W. Macdonald, Populations and activity patterns of clouded leopards and marbled cats in Dampa Tiger Reserve, India. J. Mammal. 98, 1453–1462 (2017).
- O. R. Bininda-Emonds, J. L. Gittleman, A. Purvis, Building large trees by combining phylogenetic information: A complete phylogeny of the extant Carnivora (Mammalia). *Biol. Rev.* 74, 143–175 (1999).
- K. Liakath-Ali, V. E. Vancollie, E. Heath, D. P. Smedley, J. Estabel, D. Sunter, T. DiTommaso, J. K. White, R. Ramirez-Solis, I. Smyth, Novel skin phenotypes revealed by a genome-wide mouse reverse genetic screen. *Nat. Commun.* 5, 1–13 (2014).
- G. Hua, J. Chen, J. Wang, J. Li, X. Deng, Genetic basis of chicken plumage color in artificial population of complex epistasis. *Anim. Genet.* 52, 656–666 (2021).
- C. J. Andrews, D. G. Thomas, J. Yapura, M. A. Potter, Reproductive biology of the 38 extant felid species: A review. Mammal Rev. 49, 16–30 (2019).
- C. Van Oosterhout, Transposons in the MHC: The Yin and Yang of the vertebrate immune system. Heredity 103, 190–191 (2009).
- M. Okano, J. Miyamae, S. Suzuki, K. Nishiya, F. Katakura, J. K. Kulski, T. Moritomo, T. Shiina, Identification of novel alleles and structural haplotypes of major histocompatibility complex class I and *DRB* genes in domestic cat (*Felis catus*) by a newly developed NGSbased genotyping method. *Front. Genet.* 11, 750 (2020).
- K. Wilczynska, P. Radwan, R. Krasinski, M. Radwan, J. R. Wilczynski, A. Malinowski, E. Barcz, I. Nowak, KIR and HLA-C genes in male infertility. J. Assist. Reprod. Genet. 37, 2007–2017 (2020).
- Y. Xue, J. Prado-Martinez, P. H. Sudmant, V. Narasimhan, Q. Ayub, M. Szpak, P. Frandsen, Y. Chen, B. Yngvadottir, D. N. Cooper, Mountain gorilla genomes reveal the impact of longterm population decline and inbreeding. *Science* 348, 242–245 (2015).
- D. H. Alexander, J. Novembre, K. Lange, Fast model-based estimation of ancestry in unrelated individuals. Genome Res. 19, 1655–1664 (2009).
- P. Waskova-Arnostova, B. Elsnicova, D. Kasparova, D. Hornikova, F. Kolar, J. Novotny, J. Zurmanova, Cardioprotective adaptation of rats to intermittent hypobaric hypoxia is accompanied by the increased association of hexokinase with mitochondria. J. Appl. Physiol. 119, 1487–1493 (2015).
- X. Wu, B. Bowers, K. Rao, Q. Wei, J. A. Hammer III, Visualization of melanosome dynamics within wild-type and dilute melanocytes suggests a paradigm for myosin V function in vivo. J. Cell Biol. 143, 1899–1918 (1998).
- H. Zhang, Z. Wu, L. Yang, Z. Zhang, H. Chen, J. Ren, Novel mutations in the Myo5 a gene cause a dilute coat color phenotype in mice. FASEB J. 35, e21261 (2021).
- K. Delhey, A review of Gloger's rule, an ecogeographical rule of colour: Definitions, interpretations and evidence. Biol. Rev. 94, 1294–1316 (2019).
- E. M. Lodder, P. De Nittis, C. D. Koopman, W. Wiszniewski, C. F. M. de Souza, N. Lahrouchi, N. Guex, V. Napolioni, F. Tessadori, L. Beekman, GNB5 mutations cause an autosomal-recessive multisystem syndrome with sinus bradycardia and cognitive disability. Am. J. Human Genet. 99, 704–710 (2016).
- C. C. Veerman, I. Mengarelli, C. D. Koopman, R. Wilders, S. C. van Amersfoorth, D. Bakker, R. Wolswinkel, M. Hababa, T. P. de Boer, K. Guan, Genetic variation in *GNB5* causes bradycardia by augmenting the cholinergic response via increased acetylcholine-activated potassium current (I_{K, ACh}). *Dis. Model Mech.* 12, dmm037994 (2019).
- F. L. Sciacca, C. Ciaccio, F. Fontana, C. Strano, F. Gilardoni, C. Pantaleoni, S. D'Arrigo, Severe phenotype in a patient with homozygous 15q21.2 microdeletion involving *BCL2L10*, *GNB5*, and *MYO5C* genes, resembling infantile developmental disorder with cardiac arrhythmias (IDDCA). *Front. Genet.* 11, 399 (2020).
- E. Stuchlík, D. Vondrák, Z. Hořická, J. Hrubá, A. Mijovilovich, G. Kletetschka, Identification of the younger Dryas onset was confused by the Laacher see volcanic eruption. *Proc. Natl. Acad. Sci. U.S.A.* 118, e2022485118 (2021).
- M. A. Contín, M. M. Benedetto, M. L. Quinteros-Quintana, M. E. Guido, Light pollution: The possible consequences of excessive illumination on retina. Eye 30, 255–263 (2016).
- M. Kolmogorov, J. Yuan, Y. Lin, P. A. Pevzner, Assembly of long, error-prone reads using repeat graphs. *Nat. Biotechnol.* 37, 540–546 (2019).
- J. Hu, J. Fan, Z. Sun, S. Liu, NextPolish: A fast and efficient genome polishing tool for longread assembly. *Bioinformatics* 36, 2253–2255 (2020).
- D. Guan, S. A. McCarthy, J. Wood, K. Howe, Y. Wang, R. Durbin, Identifying and removing haplotypic duplication in primary genome assemblies. *Bioinformatics* 36, 2896–2898 (2020).
- N. C. Durand, M. S. Shamim, I. Machol, S. S. Rao, M. H. Huntley, E. S. Lander, E. L. Aiden, Juicer provides a one-click system for analyzing loop-resolution hi-C experiments. *Cell Syst.* 3, 95–98 (2016).
- O. Dudchenko, S. S. Batra, A. D. Omer, S. K. Nyquist, M. Hoeger, N. C. Durand, M. S. Shamim, I. Machol, E. S. Lander, A. P. Aiden, De novo assembly of the Aedes aegypti genome using hi-C yields chromosome-length scaffolds. *Science* 356, 92–95 (2017).

SCIENCE ADVANCES | RESEARCH ARTICLE

- N. C. Durand, J. T. Robinson, M. S. Shamim, I. Machol, J. P. Mesirov, E. S. Lander, E. L. Aiden, Juicebox provides a visualization system for hi-C contact maps with unlimited zoom. *Cell Syst.* 3. 99–101 (2016).
- J. Keilwagen, M. Wenk, J. L. Erickson, M. H. Schattat, J. Grau, F. Hartung, Using intron position conservation for homology-based gene prediction. *Nucleic Acids Res.* 44, e89 (2016).
- E. Birney, M. Clamp, R. Durbin, GeneWise and genomewise. Genome Res. 14, 988–995 (2004).
- M. Stanke, O. Keller, I. Gunduz, A. Hayes, S. Waack, B. Morgenstern, AUGUSTUS: Ab initio prediction of alternative transcripts. *Nucleic Acids Res.* 34, W435–W439 (2006).
- W. H. Majoros, M. Pertea, S. L. Salzberg, TigrScan and GlimmerHMM: Two open source ab initio eukaryotic gene-finders. *Bioinformatics* 20, 2878–2879 (2004).
- 71. I. Korf, Gene finding in novel genomes. BMC Bioinformatics 5, 59 (2004).
- M. C. Frith, M. Hamada, P. Horton, Parameters for accurate genome alignment. BMC Bioinformatics 11. 1–14 (2010).
- M. Blanchette, W. J. Kent, C. Riemer, L. Elnitski, A. F. Smit, K. M. Roskin, R. Baertsch, K. Rosenbloom, H. Clawson, E. D. Green, Aligning multiple genomic sequences with the threaded blockset aligner. *Genome Res.* 14, 708–715 (2004).
- A. Stamatakis, RAxML version 8: A tool for phylogenetic analysis and post-analysis of large phylogenies. Bioinformatics 30, 1312–1313 (2014).
- Z. Yang, PAML 4: Phylogenetic analysis by maximum likelihood. Molec. Biol. Evol. 24, 1586–1591 (2007).
- A. Löytynoja, Phylogeny-aware alignment with PRANK. Methods Mol. Biol. 1079, 155–170 (2014).
- T. De Bie, N. Cristianini, J. P. Demuth, M. W. Hahn, CAFE: A computational tool for the study of gene family evolution. *Bioinformatics* 22, 1269–1271 (2006).
- Y. Zhou, B. Zhou, L. Pache, M. Chang, A. H. Khodabakhshi, O. Tanaseichuk, C. Benner,
 K. Chanda, Metascape provides a biologist-oriented resource for the analysis of systems-level datasets. *Nat. Commun.* 10, 1–10 (2019).
- H. Li, R. Durbin, Fast and accurate long-read alignment with Burrows–Wheeler transform. Bioinformatics 26, 589–595 (2010).
- A. McKenna, M. Hanna, E. Banks, A. Sivachenko, K. Cibulskis, A. Kernytsky, K. Garimella,
 D. Altshuler, S. Gabriel, M. Daly, The genome analysis toolkit: A MapReduce framework for analyzing next-generation DNA sequencing data. *Genome Res.* 20, 1297–1303 (2010).
- M. Malinsky, M. Matschiner, H. Svardal, Dsuite-fast D-statistics and related admixture evidence from VCF files. Mol. Ecol. Resour. 21, 584–595 (2021).
- E. Y. Durand, N. Patterson, D. Reich, M. Slatkin, Testing for ancient admixture between closely related populations. *Molec. Biol. Evol.* 28, 2239–2252 (2011).
- S. Purcell, B. Neale, K. Todd-Brown, L. Thomas, M. A. Ferreira, D. Bender, J. Maller, P. Sklar, P. I. De Bakker, M. J. Daly, PLINK: A tool set for whole-genome association and population-based linkage analyses. *Am. J. Human Genet.* 81, 559–575 (2007).
- 84. H. Li, R. Durbin, Inference of human population history from individual whole-genome sequences. *Nature* **475.** 493–496 (2011).
- S. Schiffels, K. Wang, MSMC and MSMC2: The multiple sequentially markovian coalescent. Methods Mol. Biol. 2090, 147–166 (2020).
- K. Tamura, G. Stecher, S. Kumar, MEGA11: Molecular evolutionary genetics analysis version 11. Molec. Biol. Evol. 38, 3022–3027 (2021).
- C. Zhang, S.-S. Dong, J.-Y. Xu, W.-M. He, T.-L. Yang, PopLDdecay: A fast and effective tool for linkage disequilibrium decay analysis based on variant call format files. *Bioinformatics* 35, 1786–1788 (2019).
- 88. E. E. Armstrong, R. W. Taylor, D. E. Miller, C. B. Kaelin, G. S. Barsh, E. A. Hadly, D. Petrov, Long live the king: Chromosome-level assembly of the lion (*Panthera leo*) using linked-read, Hi-C, and long-read data. *BMC Biol.* 18, 3 (2020).
- Y. S. Cho, L. Hu, H. Hou, H. Lee, J. Xu, S. Kwon, S. Oh, H.-M. Kim, S. Jho, S. Kim, Y.-A. Shin, B. C. Kim, H. Kim, C.-U. Kim, S.-J. Luo, W. E. Johnson, K.-P. Koepfli, A. Schmidt-Küntzel, J. A. Turner, L. Marker, C. Harper, S. M. Miller, W. Jacobs, L. D. Bertola, T. H. Kim, S. Lee, Q. Zhou, H.-J. Jung, X. Xu, P. Gadhvi, P. Xu, Y. Xiong, Y. Luo, S. Pan, C. Gou, X. Chu, J. Zhang, S. Liu, J. He, Y. Chen, L. Yang, Y. Yang, J. He, S. Liu, J. Wang, C. H. Kim, H. Kwak, J.-S. Kim, S. Hwang, J. Ko, C.-B. Kim, S. Kim, D. Bayarlkhagva, W. K. Paek, S.-J. Kim, S. J. O'Brien, J. Wang,

- J. Bhak, The tiger genome and comparative analysis with lion and snow leopard genomes.

 Nat. Commun. 4. 2433 (2013).
- S. Kim, Y. S. Cho, H.-M. Kim, O. Chung, H. Kim, S. Jho, H. Seomun, J. Kim, W. Y. Bang, C. Kim, J. An, C. H. Bae, Y. Bhak, S. Jeon, H. Yoon, Y. Kim, J. H. Jun, H. J. Lee, S. Cho, O. Uphyrkina, A. Kostyria, J. Goodrich, D. Miquelle, M. Roelke, J. Lewis, A. Yurchenko, A. Bankevich, J. Cho, S. Lee, J. S. Edwards, J. A. Weber, J. Cook, S. Kim, H. Lee, A. Manica, I. Lee, S. J. O'Brien, J. Bhak, J.-H. Yeo, Comparison of carnivore, omnivore, and herbivore mammalian genomes with a new leopard assembly. *Genome Biol.* 17, 211 (2016).
- E. E. Armstrong, A. Khan, R. W. Taylor, A. Gouy, G. Greenbaum, A. Thiéry, J. T. Kang,
 A. Redondo, S. Prost, G. Barsh, C. Kaelin, S. Phalke, A. Chugani, M. Gilbert, D. Miquelle,
 A. Zachariah, U. Borthakur, A. Reddy, E. Louis, O. A. Ryder, Y. V. Jhala, D. Petrov, L. Excoffier,
 E. Hadly, U. Ramakrishnan, Recent evolutionary history of tigers highlights contrasting
 roles of genetic drift and selection. *Molec. Biol. Evol.* 38, 2366–2379 (2021).
- P. Pěnerová, G. Garcia-Erill, X. Liu, C. Nursyifa, R. K. Waples, C. G. Santander, L. Quinn,
 P. Frandsen, J. Meisner, F. F. Stæger, M. S. Rasmussen, A. Brüniche-Olsen, C. H. F. Jørgensen,
 R. R. da Fonseca, H. R. Siegismund, A. Albrechtsen, R. Heller, I. Moltke, K. Hanghøj, High
 genetic diversity and low differentiation reflect the ecological versatility of the African
 leopard. Curr. Biol. 31, 1862–1871. e1865 (2021).
- N. F. Saremi, M. A. Supple, A. Byrne, J. A. Cahill, L. L. Coutinho, L. Dalén, H. V. Figueiró, W. E. Johnson, H. J. Milne, S. J. O'Brien, Puma genomes from north and South America provide insights into the genomic consequences of inbreeding. *Nat. Commun.* 10, 4769 (2019).
- M. Lucena-Perez, E. Marmesat, D. Kleinman-Ruiz, B. Martínez-Cruz, K. Węcek, A. P. Saveljev, I. V. Seryodkin, I. Okhlopkov, M. G. Dvornikov, J. Ozolins, Genomic patterns in the widespread Eurasian lynx shaped by Late Quaternary climatic fluctuations and anthropogenic impacts. Mol. Ecol. 29, 812–828 (2020).

Acknowledgments: We acknowledge National Museums Scotland for making the tissue samples of MCLs available through CryoArks (supported by BBSRC grant BB/R015260/1), and Guangzhou Zoo for providing the tissue sample for clouded leopard's genome sequencing and assembly. We would like to thank K. Shao from Dali University for painting the pictures of clouded leopards. We would also like to thank National Engineering Laboratory for Resource Developing of Endangered Chinese Crude Drugs in Northwest China, Shaanxi Normal University. Funding: This work was supported by the National Natural Science Foundation of China 31970391 (to G.L.), the Natural Science Basic Research Program of Shaanxi 2020JM-280 (to G.L.), Fundamental Research Funds for the Central Universities GK201902008 (to G.L.) and 2020TS054 (to J.Y.), and National Science Foundation grant DEB-1753760 (to W.J.M.). Author contributions: G.L. designed and supervised the project, A.C.K., W.C., and C.W. prepared the samples. J.Y. and L.Z. performed the genome assembly and annotations. J.Y., C.H., X.X., and L.X. carried out the comparative genomic analysis, J.Y., G.W., T.S., and C.H. performed population diversity analysis and prepared graphs. J.Y., J.W., and H.L. supported the methodology and the software. G.L., and J.Y. wrote the primary manuscript. G.L., A.C.K., Q.J., W.J.M., and D.W. edited and revised the manuscript. All of the authors discussed the results and commented on the manuscript. The author(s) read and approved the final manuscript. Competing interests: The authors declare that they have no competing interests. Data and materials availability: Raw FASTQ sequences have been deposited to NCBI Short Read Archive and genome assembly of clouded leopards under the BioProject accession number PRJNA914225, and the access number of genome assembly is JASWHX00000000. The datasets generated and analyzed during the current study are available in the main text or the Supplementary Materials. Codes for performing comparative genomic analysis and population analysis are available on GitHub repository (https://github.com/GanglabSnnu) and Zenodo (https://doi.org/10.5281/zenodo. 8132005). All data needed to evaluate the conclusions in the paper are present in the paper and/or the Supplementary Materials.

Submitted 22 March 2023 Accepted 6 September 2023 Published 6 October 2023 10.1126/sciadv.adh9143

Downloaded from https://www.science.org on November 05, 2023

Science Advances

How genomic insights into the evolutionary history of clouded leopards inform their conservation

Jiaqing Yuan, Guiqiang Wang, Le Zhao, Andrew C. Kitchener, Ting Sun, Wu Chen, Chen Huang, Chen Wang, Xiao Xu, Jinhong Wang, Huimeng Lu, Lulu Xu, Qigao Jiangzuo, William J. Murphy, Dongdong Wu, and Gang Li

Sci. Adv. 9 (40), eadh9143. DOI: 10.1126/sciadv.adh9143

View the article online

https://www.science.org/doi/10.1126/sciadv.adh9143 **Permissions**

https://www.science.org/help/reprints-and-permissions

Use of this article is subject to the Terms of service